Hindawi
Complexity
Volume 2021, Article ID 6660857, 14 pages
https://doi.org/10.1155/2021/6660857

Research Article

Robust H_∞ Feedback Compensator Design for Linear Parabolic DPSs with Pointwise/Piecewise Control and Pointwise/Piecewise Measurement

Liu Yaqiang,[1] **Ren Zhigang**,[2] **and Jin Zengwang**[3,4]

[1]*School of Automation and Guangdong-HongKong-Macao Joint Laboratory for Smart Discrete Manufacturing, Guangdong University of Technology, Guangzhou, Guangdong 510006, China*
[2]*School of Automation and Guangdong Discrete Manufacturing KnowledgeAutomation Engineering Technology Research Center, Guangdong University of Technology, Guangzhou, Guangdong 510006, China*
[3]*School of Cybersecurity, Northwestern Polytechnical University, Xi'an, Shanxi 710072, China*
[4]*National Engineering Laboratory for Integrated Aero-Space-Ground-Ocean Big Data Application Technology, Xi'an, Shanxi 710072, China*

Correspondence should be addressed to Jin Zengwang; jin_zengwang@nwpu.edu.cn

Received 19 November 2020; Revised 19 February 2021; Accepted 24 March 2021; Published 12 April 2021

Academic Editor: Xue-bo Jin

In this paper, a robust H_∞ control problem of a class of linear parabolic distributed parameter systems (DPSs) with pointwise/piecewise control and pointwise/piecewise measurement has been investigated via the robust H_∞ feedback compensator design approach. A unified Lyapunov direct approach is proposed in consideration of the pointwise/piecewise control and point/piecewise measurement based on the distributions of the actuators and sensors. A new type of Luenberger observer is developed on the continuous interval of space domain to track the state of the system, and an H_∞ performance constraint with prescribed H_∞ attenuation levels is proposed in this paper. By utilizing Lyapunov technique, mathematical inequalities, and integration theory, a sufficient condition based on LMI for the exponential stability of the corresponding closed-loop coupled system under an H_∞ performance constraint is presented. Finally, the effectiveness of the proposed design method is verified by numerical simulation results.

1. Introduction

Distributed parameter systems (DPSs) are infinite-dimensional in nature and are generally modeled by partial differential equations (PDEs). DPSs are widely used in engineering systems [1–4], such as thermodynamics, chemical engineering, missile, aerospace, aviation, and nuclear fission and fusion. Control problem of DPSs has attracted extensive attention due to the important applications in engineering systems, such as the vibration control of flexible structures that the vibration process can be described by Euler–Bernoulli equations, the diffusion control of oil spill that the diffusion phenomena can be described by diffusion equations, and the temperature control of heating furnace that the thermal conduction process can be described by heat equations. In recent decades, fruitful achievements in the design of DPSs control have been achieved from many scholars all over the world [5–17].

Generally, control forms of DPSs can be divided into boundary control and in-domain control based on the actuators' location. Fruitful achievements on boundary control of DPSs that the actuators are located at the boundary area have been published already. For example, the boundary control problem of flexible robot manipulators has been developed to solve the DPSs with flexible structures [18–20]. This technique has been extended to the boundary anti-disturbance control and boundary adaptive robust control for flexible DPSs [21–23]. Boundary control of $1D$ nonlinear

parabolic DPSs has been studied in [24], in which the continuum backstepping method is utilized. Boundary feedback control of DPSs has been addressed in [25], and a novel combination of feedback idea and backstepping approach is presented in [26]. Sampled-data boundary control and sliding mode boundary control of DPSs have been studied in [27, 28], where a sampled-data strategy for the boundary control problem is proposed. Fuzzy boundary control based on the T-S fuzzy DPS model is shown in [29, 30]. H_∞ boundary control has been proposed in [31] that a linear matrix inequality (LMI) approach has been utilized. Meanwhile, there are also some achievements on in-domain control of DPSs. For example, pointwise control of DPSs with T-S fuzzy DPS model has been developed in [32], where a fuzzy state feedback controller is designed. Furthermore, this technique has been extended to the [33, 34]. Robust sampled-data control has been proposed in [35, 36], where the sampled-data pointwise controller method is applied. Mobile piecewise control of $1D$ DPSs has been studied in [37] that a mobile actuator-plus-sensor network is developed, and this technique has been extended to solve the $2D$ DPSs in [38]. More recently, collocated control and noncollocated control of in-domain control in DPSs have been studied deeply. Static collocated feedback control has been presented in [39, 40] that the static collocated pointwise and piecewise feedback controller has been designed for parabolic DPSs. For the noncollocated control that the actuators and sensors can never be placed at the same location exactly, the static feedback control has been studied in [32, 36, 41, 42], and the observer-based dynamic feedback control has been designed in [43–47]. The estimation problems in controller design of DPSs have been studied in [48–53], and for some DPSs with unknown parameters, parameter estimation methods have been applied in [54–58].The design and analysis methods have also been extended to switched control systems and filtering technique in [59–62]. Although there have been many promising efforts, there are still many control problems of DPSs need to be studied in the future.

In general, disturbance problems of DPSs are unavoidable because of the errors from model calculations and equipments. Thus, an approach of robust H_∞ control is proposed to deal with the control problem of DPSs with external disturbances. The robust H_∞ control has attracted much attention from many scholars over the past few decades. For example, an H_∞ static output feedback boundary controller for semilinear parabolic and hyperbolic DPSs is proposed in [31]. This idea has extended to solve the sampled-data distributed H_∞ control problem for a class of parabolic DPSs in [35]. An H_∞ fuzzy observer-based controller is proposed for a class of nonlinear parabolic DPSs in [63], and this technique has developed to the observer-based H_∞ sampled-data fuzzy control design in [46, 64] and mixed H_2/H_∞ fuzzy observer-based feedback control design in [65]. In this paper, we will extend the works in [66, 67] to design the H_∞ output feedback compensator for linear parabolic DPSs with external disturbances by using a unified Lyapunov approach. A sufficient condition for the static H_∞ feedback compensator can stabilize the DPSs under an H_∞ performance constraint with the collocated observation case which is first proposed in terms of standard linear matrix inequalities (LMIs); then, another sufficient condition for the observer-based dynamic H_∞ feedback compensator can stabilize the DPSs under an H_∞ performance constraint with the noncollocated observation case which is developed by using the Lyapunov direct method, Poincaré–Wirtinger inequality's variants, Cauchy–Schwartz inequality, integration by parts, and first mean value theorem for definite integrals.

The main contributions and novelty of this paper compared with the existing works before are summarized as follows:

(i) Different from the results in [32–34, 43, 44] that the pointwise/piecewise control and collocated (or noncollocated) pointwise/piecewise measurement are discussed separately, all the forms of control and observation are considered in this paper by a unified Lyapunov direct approach.

(ii) In contrast to the works in [66] that a unified Lyapunov-based compensator design for linear parabolic DPSs with free disturbance, this paper presents the static and dynamic robust H_∞ output feedback compensator design for linear DPSs with external disturbances. Meanwhile, a new type of Luenberger observer is designed for noncollocated observation in space with continuous observation functions.

(iii) An H_∞ performance constraint in the sense of $|\cdot|_2$ is proposed to deal with the external disturbance of the model and measurement disturbance in the measurement output.

The organizational structure of the remaining parts of this paper is arranged as follows: first, the problem formulation of this paper and some preliminary knowledge are presented in Section 2. Then, the static output feedback compensator design and observer-based dynamic output feedback compensator design in terms of collocated and noncollocated observation in space satisfying the H_∞ performance constraint are shown in Section 3. Section 4 provides some numerical simulation results of the corresponding closed-loop systems to show the effectiveness of the proposed design method. Finally, brief conclusions are followed in Section 5.

Notation: $\mathfrak{R}$, $\mathfrak{R}^m$, and $\mathfrak{R}^{m\times n}$ denote the set of all real numbers, m-dimensional Euclidean space, and the set of all $m\times n$ matrices, respectively. $\mathscr{H}\triangleq\mathscr{L}^2([0,L])$ is a real Hilbert space of square integrable functions with the inner product induced norm $|\cdot|_2$. $\mathscr{L}^2([0,\infty];\mathscr{H})$ is a real Hilbert space of square integrable functions $\varpi(\cdot,t)$ with $\|\varpi\|_{\mathscr{L}_2}\triangleq\int_0^\infty|\varpi(\cdot,t)|_2\,\mathrm{d}t$. $\mathscr{L}^2([0,\infty];\mathfrak{R}^n)$ is a real Hilbert space of square integrable functions $\zeta(t)$ with $\|\zeta\|_{\mathscr{L}_2}\triangleq\int_0^\infty\|\zeta(t)\|\mathrm{d}t$. $u_t(z,t)$ stands for the partial derivative of $u(z,t)$ with respect to t, i.e., $u_t(z,t)=\partial u(z,t)/\partial t$, $u_z(z,t)$, and $u_{zz}(z,t)$ stands for the first-order and second-order partial derivative of $u(z,t)$ with respect to z, i.e., $u_z(z,t)=\partial u(z,t)/\partial z$, $u_{zz}(z,t)=\partial^2 u(z,t)/\partial z^2$, respectively. $\mathscr{M}$ and $\mathscr{N}$ denote two sets of natural numbers, i.e., $\mathscr{M}\triangleq\{1,2,\ldots,m\}$, $\mathscr{N}\triangleq\{1,2,\ldots,n\}$.

2. Problem Formulation and Preliminaries

In this paper, we consider a class of one-dimensional linear parabolic DPSs with external disturbances of the following form:

$$\begin{cases} u_t(z,t) = u_{zz}(z,t) + \eta u(z,t) + d(z,t) \\ +\mathbf{h}^T(z)\mathbf{U}(t), \quad z \in (0,L), \\ \mathbf{y}(t) = \int_0^L \mathbf{s}(z)u(z,t)\mathrm{d}z + \boldsymbol{\omega}(t), \end{cases} \tag{1}$$

subject to the Robin boundary conditions in one dimension,

$$\begin{aligned} u_z(z,t)|_{z=0} &= a_1 u(0,t), \\ u_z(z,t)|_{z=L} &= -a_2 u(L,t), \end{aligned} \tag{2}$$

and the initial condition,

$$u(z,0) = u_0(z), \quad z \in [0,L], \tag{3}$$

where $z \in [0,L] \subset \mathfrak{R}$ denotes the spatial position between $[0,L]$, and $t \geq 0$ denotes time, respectively. $u(\cdot,t) \triangleq \{u(z,t), z \in [0,L]\} \in \mathscr{H}$, denotes the state variable. $\eta > 0$ is a known constant. $d(\cdot,\cdot) \triangleq \{d(z,t), z \in [0,L]\} \in \mathscr{L}^2([0,\infty],\mathscr{H})$ is an unknown bounded external disturbance and satisfies $\int_0^\infty |d(\cdot,t)|_2^2 \mathrm{d}t < \infty$. $\mathbf{h}(z) \triangleq [\, h(z) \;\; h_2(z) \cdots h_m(z)]^T \in \mathfrak{R}^m$ is a known integrable vector function of z, and the element $h_i(z)$ describes the distribution of i-th actuator on the spatial domain $[0,L]$. $\mathbf{U}(t)$ is a set of control inputs from m actuators, expressed as $\mathbf{U}(t) \triangleq [\, u_1(t) \;\; u_2(t) \;\; \cdots \;\; u_m(t)\,]^T \in \mathfrak{R}^m$. $\mathbf{y}(t)$ is a set of measurement outputs from n sensors, expressed as $\mathbf{y}(t) \triangleq [\, y_1(t) \;\; y_2(t) \;\; \cdots \;\; y_n(t)\,]^T \in \mathfrak{R}^n$. $\mathbf{s}(z) \triangleq [\, s_1(z) \;\; s_2(z) \cdots s_n(z)]^T \in \mathfrak{R}^n$ is a known integrable vector function of z, and the element $s_j(z)$ describes the distribution of j-th sensor on the spatial domain $[0,L]$. $\omega(\cdot) \triangleq [\, \omega_1(t) \;\; \omega_2(t) \;\; \cdots \;\; \omega_n(t)\,]^T \in \mathscr{L}^2([0,\infty];\mathfrak{R}^n)$ is the n-dimensional bounded measurement disturbance vector. It should be pointed out that when $\eta > 0.25\pi^2 L^{-2}$, the one-dimensional linear parabolic DPSs is unstable.

Remark 1. It is worth noting that equation (1) is equivalent to the following general form [68]:

$$\begin{aligned} \overline{u}_t(z,t) = {} & \overline{u}_{zz}(z,t) + 2f_z(z,t)\overline{u}_z(z,t) \\ & + \left(\eta + f_z^2(z,t) + f_{zz}(z,t) - f_t(z,t)\right)\overline{u}(z,t) \\ & + d(z,t) + \overline{h}^T(z)\overline{U}(t), \quad z \in (0,L), \end{aligned} \tag{4}$$

through the conversion of the following state variables and control variables:

$$\begin{cases} f(z,t) = f_1(z) + f_2(t), \\ \overline{u}(z,t) = \exp(-f(z,t))u(z,t), \\ \overline{\mathbf{h}}^T(z) = \exp(-f_1(z))\mathbf{h}^T(z), \\ \overline{\mathbf{U}}(t) = \exp(-f_2(t))\mathbf{U}(t), \end{cases} \tag{5}$$

where $f(\cdot,t) \triangleq \{f(z,t)\} \in \mathscr{H}^2(0,L)$ is a known scalar function and continuously differentiable in time t.

In practical applications of DPSs, the number of actuators and sensors is usually limited and actives at specified point or part thereof in the spatial domain, respectively. Therefore, the in-domain control forms of DPSs are generally divided into pointwise control and local piecewise control according to the distribution of actuators. In this paper, two forms of in-domain control are both considered; the actuators' spatial distribution functions $h_i(z)$ are described as follows:

$$h_i(z) \triangleq \delta(z - \overline{z}_i), \quad i \in \mathscr{M} \text{ (pointwise control case)}, \tag{6}$$

$$h_i(z) \triangleq \begin{cases} 1 & z \in [\overline{z}_i^-, \overline{z}_i^+] \\ 0 & \text{elsewhere} \end{cases}, \quad i \in \mathscr{M} \text{ (local piecewise control case)}, \tag{7}$$

where $\delta(\cdot)$ is the Dirac delta function [69]. The points $\overline{z}_i, i \in \mathscr{M}$, and local subdomains $[\overline{z}_i^-, \overline{z}_i^+], i \in \mathscr{M}$, satisfy $0 < \overline{z}_1 < \overline{z}_2 < \cdots < \overline{z}_m < L$ and $0 < \overline{z}_1^- < \overline{z}_1^+ < \overline{z}_2^- < \overline{z}_2^+ < \cdots < \overline{z}_m^- < \overline{z}_m^+ < L$, which imply the chosen functions $g_i(z), i \in \mathscr{M}$, produce pointwise control at the points $\overline{z}_i$ and local piecewise uniform control over $[\overline{z}_i^-, \overline{z}_i^+]$, respectively. Meanwhile, the spatial domain $[0,L]$ can be divided into m parts by a spatial domain decomposition approach that $0 = z_1 < z_2 \cdots < z_{m+1} = L$. The locations of the actuators for pointwise control and local piecewise control satisfy the relationships $\overline{z}_i \in (z_i, z_{i+1}), i \in \mathscr{M}$, and $[\overline{z}_i^-, \overline{z}_i^+] \subset (z_i, z_{i+1})$, $i \in \mathscr{M}$.

Similar to the actuators' distribution, the in-domain observation forms are generally divided into pointwise measurement and local piecewise measurement; the sensors' spatial distribution functions $s_j(z), j \in \mathscr{N}$ are described in this paper as follows:

$$s_j(z) \triangleq \delta(z - \widetilde{z}_j), \quad j \in \mathscr{N} \text{ (pointwise measurement case)}, \tag{8}$$

$$s_j(z) \triangleq \begin{cases} 1 & z \in [\widetilde{z}_j^-, \widetilde{z}_j^+] \\ 0 & \text{elsewhere} \end{cases}, \quad j \in \mathscr{N} \text{ (local piecewise measurement case)}. \tag{9}$$

The points $\tilde{z}_j, j \in \mathcal{N}$, and local subdomains $[\tilde{z}_j^-, \tilde{z}_j^+], j \in \mathcal{N}$ satisfy $0 < \tilde{z}_1 < \tilde{z}_2 < \cdots < \tilde{z}_n < L$ and $0 < \tilde{z}_1^- < \tilde{z}_1^+ < \tilde{z}_2^- < \tilde{z}_2^+ < \cdots < \tilde{z}_n^- < \tilde{z}_n^+ < L$, which imply the chosen functions $c_j(z), j \in \mathcal{N}$ produce pointwise observation at the points $\tilde{z}_j$ and local piecewise uniform observation over $[\tilde{z}_j^-, \tilde{z}_j^+]$, respectively. At the same time, the spatial domain $[0, L]$ can be divided into n parts by a spatial domain decomposition approach that $0 = \hat{z}_1 < \hat{z}_2 \cdots < \hat{z}_{n+1} = L$. The locations of the sensors for pointwise measurement and local piecewise measurement satisfy the relationships $\tilde{z}_j \in (z_j, z_{j+1}), j \in \mathcal{N}$ and $[\tilde{z}_j^-, \tilde{z}_j^+] \subset (\hat{z}_j, \hat{z}_{j+1}), j \in \mathcal{N}$.

For the linear parabolic DPS (1)–(3), the following H_∞ performance constraint is proposed under the zero initial condition $u_0(\cdot) = 0$:

$$\int_0^\infty |u(\cdot,t)|_2^2 \mathrm{d}t \le \gamma_1^2 \int_0^\infty |d(\cdot,t)|_2^2 \mathrm{d}t + \gamma_2^2 \int_0^\infty \|\boldsymbol{\omega}(t)\|^2 \mathrm{d}t, \tag{10}$$

where $\gamma_1 > 0$ and $\gamma_2 > 0$ are the prescribed H_∞ attenuation levels.

For the development of stability analysis in this paper, two exponential stability definitions in the sense of $|\cdot|_2$ of the linear parabolic DPS (1)–(3) are defined.

Definition 1. The linear parabolic DPS (1)–(3) with $\mathbf{U}(t) = 0$ and $d(\cdot,t) = 0$ is exponentially stable in the sense of $|\cdot|_2$, when there exist two constants $\varepsilon_1 \ge 1$ and $\varepsilon_2 > 0$ satisfying the expression $|u(\cdot,t)|_2 \le \varepsilon_1 |u_0(\cdot)|_2 \exp(-\varepsilon_2 t)$ for any $t \ge 0$.

Definition 2. The linear parabolic DPS (1)–(3) with the designed output feedback compensator is exponentially stable in the sense of $|\cdot|_2$ under an H_∞ performance constraint, when the corresponding closed-loop DPS with $d(\cdot,t) = 0$ and $\omega(t) = 0$ is exponentially stable in the sense of $|\cdot|_2$; meanwhile, the H_∞ performance constraint in (10) is ensured when the initial value of $u(z,t)$ is zero ($u_0(z) = 0$) and all $d(\cdot,\cdot) \in \mathcal{L}_2(0,\infty;\mathcal{H}), \omega(\cdot) \in \mathcal{L}_2(0,\infty;\mathfrak{R}^n)$.

The following lemmas are very useful for the development of the robust H_∞ compensator design in this paper.

Lemma 1 (Poincaré–Wirtinger inequality's variants). *For a scalar function $u \in \mathcal{H}^1(0,L)$, we have*

$$\begin{aligned} &\int_0^L (u(s) - u(z))^2 \mathrm{d}s \le 4\tau_1 \pi^{-2} \int_0^L \left(\frac{\mathrm{d}u(s)}{\mathrm{d}s}\right)^2 \mathrm{d}s, \\ &\int_0^L (u(s) - u_l)^2 \mathrm{d}s \le 4\tau_2 \pi^{-2} \int_0^L \left(\frac{\mathrm{d}u(s)}{\mathrm{d}s}\right)^2 \mathrm{d}s, \end{aligned} \tag{11}$$

where $z \in [0,L]$, $\tau_1 \triangleq \max\{z^2, (L-z)^2\}$, $u_l \triangleq (z_2 - z_1)^{-1} \int_{z_1}^{z_2} u(z)\mathrm{d}z$, $[z_1, z_2] \subset [0,L]$, and $\tau_2 \triangleq \max\{z_2^2, (L-z_1)^2\}$. For more detailed details, please refer to the lemma in [66].

Lemma 2 *(Cauchy–Schwartz inequality [70]). For any two scalar functions $\vartheta_1 \in \mathcal{H}^1(0,L)$ and $\vartheta_2 \in \mathcal{H}^1(0,L)$, there exists constant $\tau_3 > 0$ which makes the following inequality hold:*

$$\begin{aligned} \int_0^L \vartheta_1(z)\vartheta_2(z)\mathrm{d}s &\le \|\vartheta_1(z)\|\|\vartheta_2(z)\| \\ &\le \frac{\tau_3}{2}\|\vartheta_1(z)\|^2 + \frac{1}{2\tau_3}\|\vartheta_2(z)\|^2. \end{aligned} \tag{12}$$

3. Robust H_∞ Feedback Compensator Design

Based on the distributions of actuators and sensors that $h_i(z), i \in \mathcal{M}$, in (6) (or (7)) and $s_j(z), j \in \mathcal{N}$, in (8) (or (9)), the observation obtained from sensors can be divided into collocated observation in space (i.e., $\mathbf{h}(z) = \mathbf{s}(z)$) and noncollocated observation in space (i.e., $\mathbf{h}(z) \ne \mathbf{s}(z)$). In other words, the collocated observation in space is a special case of noncollocated observation. Meanwhile, the noncollocated observation in space (i.e., $\mathbf{h}(z) \ne \mathbf{s}(z)$) consists of the following cases: pointwise control and noncollocated pointwise observation case, pointwise control and noncollocated piecewise observation case, piecewise control and noncollocated pointwise observation case, and piecewise control and noncollocated piecewise observation case. In this section, all the noncollocated observation cases will be considered to study the robust H_∞ dynamic output feedback compensator design for the DPS (1)–(3).

A new type of Luenberger-type observer for the DPS (1)–(3) is constructed as follows:

$$\begin{cases} \hat{u}_t(z,t) = \hat{u}_{zz}(z,t) + \eta\hat{u}(z,t) + \hat{\mathbf{h}}^T(z)\mathbf{U}(t) \\ +\hat{s}^T(z)\hat{\mathbf{L}}[\mathbf{y}(t) - \hat{y}(t)], \quad t > 0, z \in (0,L), \\ \hat{u}_z(z,t)|_{z=0} = a_1\hat{u}(0,t), \\ \hat{u}_z(z,t)|_{z=L} = -a_2\hat{u}(L,t), \\ \hat{u}(z,0) = \hat{u}_0(z), \quad z \in [0,L], \\ \hat{y}(t) = \displaystyle\int_0^L \mathbf{s}(z)\hat{u}(z,t)\mathrm{d}z, \quad t \ge 0, \end{cases} \tag{13}$$

where $\hat{u}(z,t)$ denotes the state of the observer; $0 < \hat{L} \triangleq \mathrm{diag}\{l_1, l_2, \ldots, l_n\} \in \mathfrak{R}^{n\times n}$ is the observer gain to be determined.

The observation functions $\hat{s}(z) \triangleq [\hat{s}_1(z)\ \hat{s}_2(z)\ \cdots\ \hat{s}_n(z)]^T$ are choosen as

$$\hat{s}_j(z) \triangleq \begin{cases} 1 & z \in [\hat{z}_j, \hat{z}_{j+1}] \\ 0 & \text{elsewhere} \end{cases}, \quad j \in \mathcal{N}, \tag{14}$$

such that $0 = \hat{z}_1 < \hat{z}_2 < \cdots < \hat{z}_n < \hat{z}_{n+1} = L$.

Then, we design an observer-based dynamic output feedback compensator of the following form:

$$\mathbf{U}(t) = -\hat{\mathbf{K}} \int_0^L \hat{\mathbf{h}}(z)\hat{u}(z,t)\mathrm{d}z, \quad t \ge 0, \tag{15}$$

where $0 < \hat{K} \triangleq \mathrm{diag}\{k_1, k_2, \ldots, k_m\} \in \mathfrak{R}^{m\times m}$ is the compensator gain in the form of $m \times m$ diagonal matrix, and the compensator functions $\hat{h}(z) \triangleq [\hat{h}_1(z)\ \hat{h}_2(z)\ \cdots\ \hat{h}_m(z)]^T \in \mathfrak{R}^m$ are choosen as

$$\widehat{h}_i(z) \triangleq \begin{cases} 1 & z \in [z_i, z_{i+1}] \\ 0 & \text{elsewhere} \end{cases}, \quad i \in \mathscr{M}, \tag{16}$$

such that $0 = z_1 < z_2 < \cdots < z_m < z_{m+1} = L$.

The estimation error state is defined as

$$e(z,t) \triangleq u(z,t) - \widehat{u}(z,t), \quad z \in [0, L]. \tag{17}$$

From formulas (1)–(3) and (13)–(17), the estimation error system is represented as

$$\begin{cases} e_t(z,t) = e_{zz}(z,t) + \eta e(z,t) + d(z,t) \\ -\widehat{s}^T(z)\widehat{\mathbf{L}}\int_0^L \mathbf{s}(z)e(z,t)\mathrm{d}z \\ -\widehat{s}^T(z)\widehat{\mathbf{L}}\omega(t), \quad z \in (0, L), \\ e_z(z,t)|_{z=0} = a_1 e(0,t), \\ e_z(z,t)|_{z=L} = -a_2 e(L,t), \\ e(z,0) = e_0(z), \quad z \in [0, L], \end{cases} \tag{18}$$

where the initial value $e_0(z) \triangleq u_0(z) - \widehat{u}_0(z)$.

Substituting the designed dynamic feedback compensator (15) and the estimation error state (17) into the DPS (1)–(3), the following closed-loop system is obtained as follows:

$$\begin{cases} u_t(z,t) = u_{zz}(z,t) + \eta u(z,t) + d(z,t) \\ -\mathbf{h}^T(z)\widehat{\mathbf{K}}\int_0^L \widehat{\mathbf{h}}(z)u(z,t)\mathrm{d}z \\ +\mathbf{h}^T(z)\widehat{\mathbf{K}}\int_0^L \widehat{\mathbf{h}}(z)e(z,t)\mathrm{d}z, \quad z \in (0, L), \\ u_z(z,t)|_{z=0} = a_1 u(0,t), \\ u_z(z,t)|_{z=L} = -a_2 u(L,t), \\ u(z,0) = u_0(z), \quad z \in [0, L]. \end{cases} \tag{19}$$

Hence, the closed-loop coupled DPS is represented by the estimation error system (18) and the closed-loop system (19) with expressions (6) (or (7)) and (8) (or (9)). The objective of this subsection is to seek an effective method to design an observer-based dynamic output feedback compensator such that the resulting closed-loop coupled DPS is exponentially stable under an H_∞ performance constraint in the sense of $|\cdot|_2$ with prescribed H_∞ attenuation levels γ_1 and γ_2.

The following theorem provides a sufficient condition for the exponential stability of the closed-loop coupled DPS (18), (19), (6) (or (7)), and (8) (or (9)) with $d(\cdot,t) = 0, \omega(t) = 0$ in the sense of $|\cdot|_2$.

Theorem 1. *Consider a class of linear parabolic DPSs (1)–(3) with $d(\cdot,t) = 0, \omega(t) = 0$ for noncollocated observation (i.e., $\mathbf{h}(z) \neq \mathbf{s}(z)$). If there exist compensator gains k_i, $i \in \mathscr{M}$, and scalars $\widehat{l}_j$, $j \in \mathscr{N}$,satisfying the following LMI constraints:*

$$\widehat{\Pi}_i \triangleq \begin{bmatrix} \eta - \dfrac{\pi^2}{4\phi_i} & \dfrac{\pi^2\sigma_i}{4\phi_i} - \dfrac{k_i}{2} & 0 \\ \dfrac{\pi^2\sigma_i}{4\phi_i} - \dfrac{k_i}{2} & -\dfrac{\pi^2\sigma_i^2}{4\phi_i} & k_i \\ 0 & k_i & -2\varepsilon \end{bmatrix} < 0, \quad i \in \mathscr{M}, \tag{20}$$

$$\widehat{\Psi}_j \triangleq \begin{bmatrix} q\eta - \dfrac{q\pi^2}{4\varphi_j} + \dfrac{\varepsilon}{2} & \dfrac{q\pi^2\widehat{\sigma}_j}{4\varphi_j} - \dfrac{\widehat{l}_j}{2} \\ \dfrac{q\pi^2\widehat{\sigma}_j}{4\varphi_j} - \dfrac{\widehat{l}_j}{2} & -\dfrac{q\pi^2\widehat{\sigma}_j^2}{4\varphi_j} \end{bmatrix} < 0, \quad j \in \mathscr{N}, \tag{21}$$

in which

$$\widehat{\sigma}_j \triangleq \begin{cases} 1, & j \in \mathscr{N} \text{ (pointwise observation case)}, \\ \dfrac{1}{\widetilde{z}_j^R - \widetilde{z}_j^L}, & j \in \mathscr{N} \text{ (local piecewise observation case)}, \end{cases}$$

$$\varphi_j \triangleq \begin{cases} \max\left\{\left(\widehat{z}_{j+1} - \widetilde{z}_j\right)^2, \left(\widetilde{z}_j - \widehat{z}_j\right)^2\right\}, & j \in \mathscr{N} \text{ (pointwise measurement case)}, \\ \max\left\{\left(\widehat{z}_{j+1} - \widetilde{z}_j^L\right)^2, \left(\widetilde{z}_j^R - \widehat{z}_j\right)^2\right\}, & j \in \mathscr{N} \text{ (piecewise measurement case)}, \end{cases} \tag{22}$$

and then there exists an observer-based dynamic output feedback compensator (15) ensuring the exponential stability of the closed-loop coupled DPS (18), (19), (6) (or (7)), and (8) (or (9)) with $d(\cdot,t) = 0, \omega(t) = 0$ in the sense of $|\cdot|_2$.

Proof. Assume the LMIs (20) and (21) are fulfilled. Consider the following Lyapunov function candidate:

$$V(t) = V_1(t) + V_2(t), \tag{23}$$

in which

$$V_2(t) = 0.5q\int_0^L e^2(z,t)\mathrm{d}z, \tag{24}$$

where $q > 0$ is a Lyapunov parameter to be determined.

The time derivative of $V_1(t)$ for the closed-loop system (19) is

$$\begin{aligned}\dot{V}_1(t) \le & -\int_0^L u_z^2(z,t)\mathrm{d}z + \eta\int_0^L u^2(z,t)\mathrm{d}z \\ & -\int_0^L u(z,t)\mathbf{h}^T(z)\mathrm{d}z\widehat{\mathbf{K}}\int_0^L \widehat{\mathbf{h}}(z)u(z,t)\mathrm{d}z + \int_0^L u(z,t)\mathbf{h}^T(z)\mathrm{d}z\widehat{\mathbf{K}}\int_0^L \widehat{\mathbf{h}}(z)e(z,t)\mathrm{d}z \\ = & -\int_0^L u_z^2(z,t)\mathrm{d}z + \eta\int_0^L u^2(z,t)\mathrm{d}z - \sum_{i=1}^m k_i u(z_c,t)\int_{z_i}^{z_{i+1}} u(z,t)\mathrm{d}z \\ & + \sum_{i=1}^m k_i u(z_c,t)\int_{z_i}^{z_{i+1}} e(z,t)\mathrm{d}z.\end{aligned} \tag{25}$$

Based on the Cauchy–Schwartz inequality, the following inequality is fulfilled for any scalar $\varepsilon > 0$:

$$\int_{z_i}^{z_{i+1}} k_i u(z_c,t)e(z,t)\mathrm{d}z \le \frac{1}{2}\left(\varepsilon^{-1}\int_{z_i}^{z_{i+1}} k_i^2 u^2(z_c,t)\mathrm{d}z + \varepsilon\int_{z_i}^{z_{i+1}} e^2(z,t)\mathrm{d}z\right). \tag{26}$$

Due to $\overline{z}_i \in (z_i, z_{i+1})$ and $[\overline{z}_i^-, \overline{z}_i^+] \subset (z_i, z_{i+1}), i \in \mathscr{M}$, by Poincaré–Wirtinger inequality's variants in Lemma 1, the following inequality is fulfilled for each $z \in [z_i, z_{i+1}], i \in \mathscr{M}$:

$$\int_{z_i}^{z_{i+1}} u_z^2(z,t)\mathrm{d}z \ge \frac{\pi^2}{4\phi_i}\int_{z_i}^{z_{i+1}} \left(u(z,t) - \sigma_i u(z_c,t)\right)^2\mathrm{d}z. \tag{27}$$

Substituting the inequalities (27) and (26) into (25), we get

$$\begin{aligned}\dot{V}_1(t) \le & -\sum_{i=1}^m \int_{z_i}^{z_{i+1}} \frac{\pi^2}{4\phi_i}\left(u(z,t) - \sigma_i u(z_c,t)\right)^2\mathrm{d}z + \eta\sum_{i=1}^m \int_{z_i}^{z_{i+1}} u^2(z,t)\mathrm{d}z \\ & -\sum_{i=1}^m \int_{z_i}^{z_{i+1}} k_i u(z_c,t)u(z,t)\mathrm{d}z + \frac{1}{2\varepsilon}\sum_{i=1}^m \int_{z_i}^{z_{i+1}} k_i^2 u^2(z_c,t)\mathrm{d}z + \frac{\varepsilon}{2}\sum_{i=1}^m \int_{z_i}^{z_{i+1}} e^2(z,t)\mathrm{d}z \\ = & \sum_{i=1}^m \int_{z_i}^{z_{i+1}} \mathbf{u}_i^T(z,t)\Pi_i\mathbf{u}_i(z,t)\mathrm{d}z + \frac{\varepsilon}{2}\int_0^L e^2(z,t)\mathrm{d}z,\end{aligned} \tag{28}$$

where

$$\Pi_i \triangleq \begin{bmatrix} \eta - \dfrac{\pi^2}{4\phi_i} & \dfrac{\pi^2\sigma_i}{4\phi_i} - \dfrac{k_i}{2} \\ \dfrac{\pi^2\sigma_i}{4\phi_i} - \dfrac{k_i}{2} & -\dfrac{\pi^2\sigma_i^2}{4\phi_i} + \dfrac{k_i^2}{2\varepsilon} \end{bmatrix} < 0, \quad i \in \mathscr{M}. \tag{29}$$

The time derivative of $V_2(t)$ is

$$\begin{aligned}\dot{V}_2(t) \le & -q\int_0^L e_z^2(z,t)\mathrm{d}z + q\eta\int_0^L e^2(z,t)\mathrm{d}z - q\int_0^L e(z,t)\widehat{s}^T(z)\widehat{\mathbf{L}}\int_0^L \mathbf{s}(z)e(z,t)\mathrm{d}z \\ = & -q\int_0^L e_z^2(z,t)\mathrm{d}z + q\eta\int_0^L e^2(z,t)\mathrm{d}z - \sum_{j=1}^n \widehat{l}_j e(\widehat{z}_s,t)\int_{\widehat{z}_j}^{\widehat{z}_{j+1}} e(z,t)\mathrm{d}z,\end{aligned} \tag{30}$$

where $\widehat{l}_j = ql_j, e(\widehat{z}_s, t) = \int_0^L s_j(z)e(z,t)\mathrm{d}z, j \in \mathcal{N}$. The following expression is utilized by applying integration by parts and considering the boundary conditions in (18):

$$\begin{aligned}\int_0^L e(z,t)e_{zz}(z,t)\mathrm{d}z &= e(z,t)e_z(z,t)|_{z=0}^{z=L} - \int_0^L e_z^2(z,t)\mathrm{d}z \\ &= -a_2e^2(L,t) - a_1e^2(0,t) - \int_0^L e_z^2(z,t)\mathrm{d}z \\ &\le -\int_0^L e_z^2(z,t)\mathrm{d}z.\end{aligned} \tag{31}$$

As $\widetilde{z}_j \in (\widehat{z}_j, \widehat{z}_{j+1}), [\widetilde{z}_j^-, \widetilde{z}_j^+] \subset (\widehat{z}_j, \widehat{z}_{j+1}), j \in \mathcal{N}$, and $0 = \widehat{z}_1 < \widehat{z}_2 < \cdots < \widehat{z}_n < \widehat{z}_{n+1} = L$. By Lemma 1, we get for each $z \in [\widehat{z}_j, \widehat{z}_{j+1}], j \in \mathcal{N}$,

$$\int_{\widehat{z}_j}^{\widehat{z}_{j+1}} e_z^2(z,t)\mathrm{d}z \ge \frac{\pi^2}{4\varphi_j}\int_{\widehat{z}_j}^{\widehat{z}_{j+1}} \left(e(z,t) - \widehat{\sigma}_j e(\widehat{z}_s,t)\right)^2\mathrm{d}z. \tag{32}$$

Thus, the expression (30) can be rewritten as

$$\begin{aligned}\dot{V}_2(t) &\le -\frac{q\pi^2}{4\varphi_j}\sum_{j=1}^n\int_{\widehat{z}_j}^{\widehat{z}_{j+1}} \left(e(z,t) - \widehat{\sigma}_j e(\widehat{z}_s,t)\right)^2\mathrm{d}z + q\eta\sum_{j=1}^n\int_{\widehat{z}_j}^{\widehat{z}_{j+1}} e^2(z,t)\mathrm{d}z \\ &\quad - \sum_{j=1}^n\int_{\widehat{z}_j}^{\widehat{z}_{j+1}} \widehat{l}_j e(\widehat{z}_s,t)e(z,t)\mathrm{d}z \\ &= \sum_{j=1}^n\int_{\widehat{z}_j}^{\widehat{z}_{j+1}} \mathbf{e}_j^T(z,t)\Psi_j\mathbf{e}_j(z,t)\mathrm{d}z,\end{aligned} \tag{33}$$

where $\mathbf{e}_j(z,t) \triangleq [\, e(z,t) \;\; e(\widehat{z}_s,t)\,]^T, j \in \mathcal{N}$, and

$$\Psi_j \triangleq \begin{bmatrix} q\eta - \dfrac{q\pi^2}{4\varphi_j} & \dfrac{q\pi^2\widehat{\sigma}_j}{4\varphi_j} - \dfrac{\widehat{l}_j}{2} \\ \dfrac{q\pi^2\widehat{\sigma}_j}{4\varphi_j} - \dfrac{\widehat{l}_j}{2} & -\dfrac{q\pi^2\widehat{\sigma}_j^2}{4\varphi_j} \end{bmatrix} < 0, \quad j \in \mathcal{N}. \tag{34}$$

From (28) and (33), the time derivative of $V(t)$ defined in (23) is given as

$$\begin{aligned}\dot{V}(t) &= \dot{V}_1(t) + \dot{V}_2(t) \\ &\le \sum_{i=1}^m\int_{z_i}^{z_{i+1}} \mathbf{u}_i^T(z,t)\Pi_i\mathbf{u}_i(z,t)\mathrm{d}z + \frac{\varepsilon}{2}\int_0^L e^2(z,t)\mathrm{d}z + \sum_{j=1}^n\int_{\widehat{z}_j}^{\widehat{z}_{j+1}} \mathbf{e}_j^T(z,t)\Psi_j\mathbf{e}_j(z,t)\mathrm{d}z \\ &\le \sum_{i=1}^m\int_{z_i}^{z_{i+1}} \mathbf{u}_i^T(z,t)\Pi_i\mathbf{u}_i(z,t)\mathrm{d}z + \sum_{j=1}^n\int_{\widehat{z}_j}^{\widehat{z}_{j+1}} \mathbf{e}_j^T(z,t)\widehat{\Psi}_j\mathbf{e}_j(z,t)\mathrm{d}z.\end{aligned} \tag{35}$$

By the Schur complement and the LMI constraint (20), we have

$$\Pi_i < 0, \quad i \in \mathcal{M}. \tag{36}$$

It can be deduced from the LMI (21) and the inequality (36) that there exists an appropriate constant $\alpha_2 > 0$, satisfying the following inequalities:

$$\begin{aligned}\Pi_i + 0.5\alpha_2\mathbf{I} \le 0, &\quad i \in \mathcal{M}, \\ \widehat{\Psi}_j + 0.5\alpha_2\mathbf{I} \le 0, &\quad j \in \mathcal{N}.\end{aligned} \tag{37}$$

Substituting the inequalities (37) to (35), we obtain

$$\begin{aligned}\dot{V}(t) &\le -0.5\alpha_2\sum_{i=1}^m\int_{z_i}^{z_{i+1}} \mathbf{u}_i^T(z,t)\mathbf{u}_i(z,t)\mathrm{d}z \\ &\quad - 0.5\alpha_2\sum_{j=1}^n\int_{\widehat{z}_j}^{\widehat{z}_{j+1}} \mathbf{e}_j^T(z,t)\mathbf{e}_j(z,t)\mathrm{d}z \\ &\le -\alpha_2\left(V_1(t) + q^{-1}V_2(t)\right) \le -\alpha_2\kappa V(t),\end{aligned} \tag{38}$$

where $\kappa \triangleq \min\{1, q^{-1}\}$. Integrating from 0 to t for the inequality (38), we can get $V_1(t) \le V_1(0)\exp(-\alpha_1 t)$, which

implies $|u(\cdot,t)|_2 \le |u_0(\cdot)|_2 \exp(-0.5\alpha_1 t)$, $t \ge 0$. Thus, we can obtain $\sqrt{|u(\cdot,t)|_2^2 + |e(\cdot,t)|_2^2} \le \sqrt{\max\{1,q\}/\min\{1,q\}}$ $\sqrt{|u_0(\cdot)|_2^2 + |e_0(\cdot)|_2^2} \exp(-0.5\alpha_2 \kappa t)$. In other words, the closed-loop coupled DPS (18), (19), (6) (or (7)), and (8) (or (9)) with $d(\cdot,t) = 0, \omega(t) = 0$ is exponentially stable in the sense of $|\cdot|_2$. The proof is complete. □

Next, the H_∞ performance analysis is developed for the closed-loop coupled DPS (18), (19), (6) (or (7)), and (8) (or (9)) with the initial value $u_0(\cdot) = 0$ and all $d \in \mathscr{L}_2(0,\infty;\mathscr{H}), \omega \in \mathscr{L}_2(0,\infty;\mathfrak{R}^n)$. The following theorem provides a sufficient condition for exponential stability in the sense of $|\cdot|_2$ of the closed-loop coupled DPS (18), (19), (6) (or (7)), and (8) (or (9)) under a prescribed H_∞ performance constraint (10) based on the LMI conditions.

Theorem 2. *Consider a class of linear parabolic DPSs (1)–(3), given H_∞ attenuation levels $\gamma_1 > 0, \gamma_2 > 0$ and constant $0 < r < 1$, if there exist compensator gains k_i, $i \in \mathscr{M}$ and scalars $\widehat{l}_j$, $j \in \mathscr{N}$, satisfying the following LMI constraints:*

$$\widehat{\Gamma}_i \triangleq \begin{bmatrix} \mathfrak{p}_i & \mathfrak{q}_i & 0 & 0.5 \\ \mathfrak{q}_i & -\dfrac{\pi^2\sigma_i^2}{4\phi_i} & k_i & 0 \\ 0 & k_i & -2\varepsilon & 0 \\ 0.5 & 0 & 0 & -\dfrac{r\gamma_1^2}{\Delta z_i} \end{bmatrix} < 0, \quad i \in \mathscr{M}, \tag{39}$$

$$\Theta_j \triangleq \begin{bmatrix} \mathfrak{h}_j & \mathfrak{v}_j & 0.5q & -\dfrac{\widehat{l}_j}{2} \\ \mathfrak{v}_j & -\dfrac{q\pi^2\widehat{\sigma}_j^2}{4\varphi_j} & 0 & 0 \\ 0.5q & 0 & -\dfrac{(1-r)\gamma_1^2}{\Delta\widehat{z}_j} & 0 \\ -\dfrac{\widehat{l}_j}{2} & 0 & 0 & -\dfrac{\gamma_2^2}{\Delta\widehat{z}_j} \end{bmatrix} < 0, \quad j \in \mathscr{N}, \tag{40}$$

in which

$$\begin{aligned} \mathfrak{p}_i &\triangleq \eta - \frac{\pi^2}{4\phi_i} + 1, \\ \mathfrak{q}_i &\triangleq \frac{\pi^2\sigma_i}{4\phi_i} - \frac{k_i}{2}, \\ \mathfrak{h}_j &\triangleq q\eta - \frac{q\pi^2}{4\varphi_j} + \frac{\varepsilon}{2}, \\ \mathfrak{v}_j &\triangleq \frac{q\pi^2\widehat{\sigma}_j}{4\varphi_j} - \frac{\widehat{l}_j}{2}, \\ \Delta\widehat{z}_j &\triangleq \widehat{z}_{j+1} - \widehat{z}_j, \quad j \in \mathscr{N}, \end{aligned} \tag{41}$$

and then there exists an observer-based dynamic output feedback compensator (15) ensuring the exponential stability of the closed-loop coupled DPS (18), (19), (6) (or (7)), and (8) (or (9)) under a prescribed H_∞ performance constraint (10).

Proof. From expressions (18), (19), and (35), the time derivative of $V(t)$ is rewritten as

$$\begin{aligned} \dot{V}(t) \le & \sum_{i=1}^{m} \int_{z_i}^{z_{i+1}} \mathbf{u}_i^T(z,t)\Pi_i\mathbf{u}_i(z,t)\mathrm{d}z \\ & + \sum_{j=1}^{n} \int_{\widehat{z}_j}^{\widehat{z}_{j+1}} \mathbf{e}_j^T(z,t)\widehat{\Psi}_j\mathbf{e}_j(z,t)\mathrm{d}z + \int_0^L u(z,t)d(z,t)\mathrm{d}z + q\int_0^L e(z,t)d(z,t)\mathrm{d}z \\ & - \sum_{j=1}^{n} \int_{\widehat{z}_j}^{\widehat{z}_{j+1}} \widehat{l}_j\omega_j(t)e(z,t)\mathrm{d}z. \end{aligned} \tag{42}$$

Considering the H_∞ performance constraint in (10) and constant $0 < r < 1$, we have

$$\begin{aligned}
&\dot{V}(t) + |u(\cdot,t)|_2^2 - \gamma_1^2 |d(\cdot,t)|_2^2 - \gamma_2^2 \|\boldsymbol{\omega}(t)\|^2 \\
&\le \sum_{i=1}^{m} \int_{z_i}^{z_{i+1}} \mathbf{u}_i^T(z,t)\Pi_i \mathbf{u}_i(z,t)\mathrm{d}z + \sum_{j=1}^{n} \int_{\widehat{z}_j}^{\widehat{z}_{j+1}} \mathbf{e}_j^T(z,t)\widehat{\Psi}_j \mathbf{e}_j(z,t)\mathrm{d}z \\
&\quad + \int_0^L u(z,t)d(z,t)\mathrm{d}z + q\int_0^L d(z,t)e(z,t)\mathrm{d}z - \sum_{j=1}^{n} \int_{\widehat{z}_j}^{\widehat{z}_{j+1}} \widehat{l}_j \omega_j(t) e(z,t)\mathrm{d}z \\
&\quad + \sum_{i=1}^{m} \int_{z_i}^{z_{i+1}} u^2(z,t)\mathrm{d}z - \sum_{i=1}^{m} \frac{r\gamma_1^2}{\Delta z_i} \int_{z_i}^{z_{i+1}} d^2(z,t)\mathrm{d}z \\
&\quad - \sum_{j=1}^{n} \frac{(1-r)\gamma_1^2}{\Delta \widehat{z}_j} \int_{\widehat{z}_j}^{\widehat{z}_{j+1}} d^2(z,t)\mathrm{d}z - \sum_{j=1}^{n} \frac{\gamma_2^2}{\Delta \widehat{z}_j} \int_{\widehat{z}_j}^{\widehat{z}_{j+1}} \omega_j^2(t)\mathrm{d}z \\
&\le \sum_{i=1}^{m} \int_{z_i}^{z_{i+1}} \widehat{\mathbf{u}}_i^T(z,t)\Gamma_i \widehat{\mathbf{u}}_i(z,t)\mathrm{d}z + \sum_{j=1}^{n} \int_{\widehat{z}_j}^{\widehat{z}_{j+1}} \widehat{e}_j^T(z,t)\Theta_j \widehat{e}_j(z,t)\mathrm{d}z,
\end{aligned} \tag{43}$$

where $\widehat{u}_i(z,t) \triangleq \left[\, u(z,t) \;\; u(z_c,t) \;\; d(z,t) \,\right]^T, i \in \mathscr{M}$, $\widehat{e}_j(z,t) \triangleq \left[\, e(z,t) \;\; e(\widehat{z}_s,t) \;\; d(z,t) \;\; \omega_j(t) \,\right]^T, j \in \mathscr{N}$, and

$$\Gamma_i \triangleq \begin{bmatrix} \eta - \dfrac{\pi^2}{4\phi_i} + 1 & \dfrac{\pi^2\sigma_i}{4\phi_i} - \dfrac{k_i}{2} & 0.5 \\ \dfrac{\pi^2\sigma_i}{4\phi_i} - \dfrac{k_i}{2} & -\dfrac{\pi^2\sigma_i^2}{4\phi_i} + \dfrac{k_i^2}{2\varepsilon} & 0 \\ 0.5 & 0 & -\dfrac{r\gamma_1^2}{\Delta z_i} \end{bmatrix}, \quad i \in \mathscr{M}. \tag{44}$$

By the Schur complement and the LMI constraint (40), we have

$$\Gamma_i < 0, \quad i \in \mathscr{M}. \tag{45}$$

It is easily obtained from (43) in consideration of the inequality (45) and the LMI (40) that

$$\dot{V}(t) + |u(\cdot,t)|_2^2 - \gamma_1^2 |d(\cdot,t)|_2^2 - \gamma_2^2 \|\boldsymbol{\omega}(t)\|^2 \le 0, \quad \forall t \ge 0. \tag{46}$$

Intergrating (46) from 0 to ∞ and considering the zero initial value $u_0(\cdot) = 0$, we get the expression (10). In other words, the H_∞ performance constraint (10) with the given prescribed H_∞ attenuation levels $\gamma_1 > 0$ and $\gamma_2 > 0$ is guaranteed for the closed-loop coupled DPSs (18), (19), (6) (or (7)), and (8) (or (9)) with the initial value $u_0(\cdot) = 0$ and all $d \in \mathscr{L}_2(0,\infty;\mathscr{H})), \omega \in \mathscr{L}_2(0,\infty;\mathfrak{R}^n)$. Meanwhile, the LMI constraints (20) and (21) in Theorem 1 can be derived from the LMI constraints (39) and (40) in Theorem 2. Therefore, the closed-loop coupled DPS (18), (19), (6) (or (7)), and (8) (or (9)) is exponential stable in the sense of $|\cdot|_2$ under a prescribed H_∞ performance constraint (10). The proof is complete. □

4. Numerical Simulation

In this section, we will provide some numerical simulations to demonstrate the effectiveness of the proposed design strategy. For the linear parabolic DPS (1)–(3), given the constants $\eta = 3, L = 1, a_1 = 0.5$, and $a_2 = 0$, set the initial value $u_0(z) = 0.5\sin(0.5L^{-1}\pi x) + 0.5\pi, z \in [0,L]$, $d(z,t) = \cos(\pi z)\exp(-t)$, the open-loop profile of evolution of $u(z,t)$, and the open-loop trajectory of $|u(\cdot,t)|_2$, as shown in Figure 1. It is easily seen from Figure 1 that the linear parabolic DPS (1)–(3) with $\mathbf{U}(t) = 0$ is unstable.

The numerical simulations of the corresponding closed-loop coupled DPS (18), (19), (7), and (9) for local piecewise control and noncollocated local piecewise measurement case in space are then shown. Assume three actuators and two sensors are applied for implementation of the proposed design method, that is, $m = 3, n = 2$, and $\mathscr{M} = \{1,2,3\}, \mathscr{N} = \{1,2\}$. Three actuators are respectively distributed over $[0.1L, 0.3L]$, $[0.4L, 0.6L]$, and $[0.7L, 0.9L]$ over the spatial domain $[0,L]$, and two sensors are respectively distributed over $[[0.2L, 0.4L], [0.6L, 0.8L]$ over the spatial domain $[0,L]$, i.e., $\overline{z}_1^- = 0.1L$, $\overline{z}_1^+ = 0.3L$, $\overline{z}_2^- = 0.4L$, $\overline{z}_2^+ = 0.6L$, $\overline{z}_3^- = 0.7L$, $\overline{z}_3^+ = 0.9L$ and $\widetilde{z}_1^- = 0.2L, \widetilde{z}_1^+ = 0.4L, \widetilde{z}_2^- = 0.6L, \widetilde{z}_2^+ = 0.8L$, respectively. Set $z_1 = 0$, $z_2 = (L/3)$, $z_3 = (2L/3)$, and $z_4 = L$ and $\widehat{z}_1 = 0, \widehat{z}_2 = 0.5L$, and $\widehat{z}_3 = L$. Through numerical calculations, we can get $\Delta z_1 = \Delta z_2 = \Delta z_3 = (L/3)$, $\Delta\widehat{z}_1 = \Delta\widehat{z}_2 = 0.5L, \sigma_1 = \sigma_2 = \sigma_2 = 5L^{-1}, \widehat{\sigma}_1 = \widehat{\sigma}_2 = 5L^{-1}, \phi_1 = 0.09L^2, \phi_2 = 0.0711L^2, \phi_3 = 0.09L^2$, and $\varphi_1 = 0.16L^2, \varphi_2 = 0.2178L^2$. Set

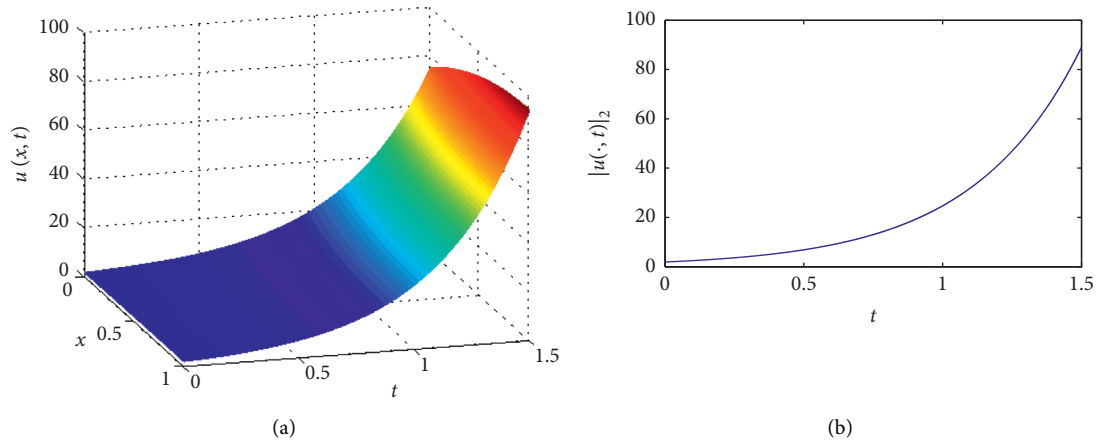

Figure 1: Simulation results for the open-loop linear parabolic DPS (1)–(3). (a) Open-loop profile of evolution of $u(z,t)$. (b) Open-loop trajectory of $|u(\cdot,t)|_2$.

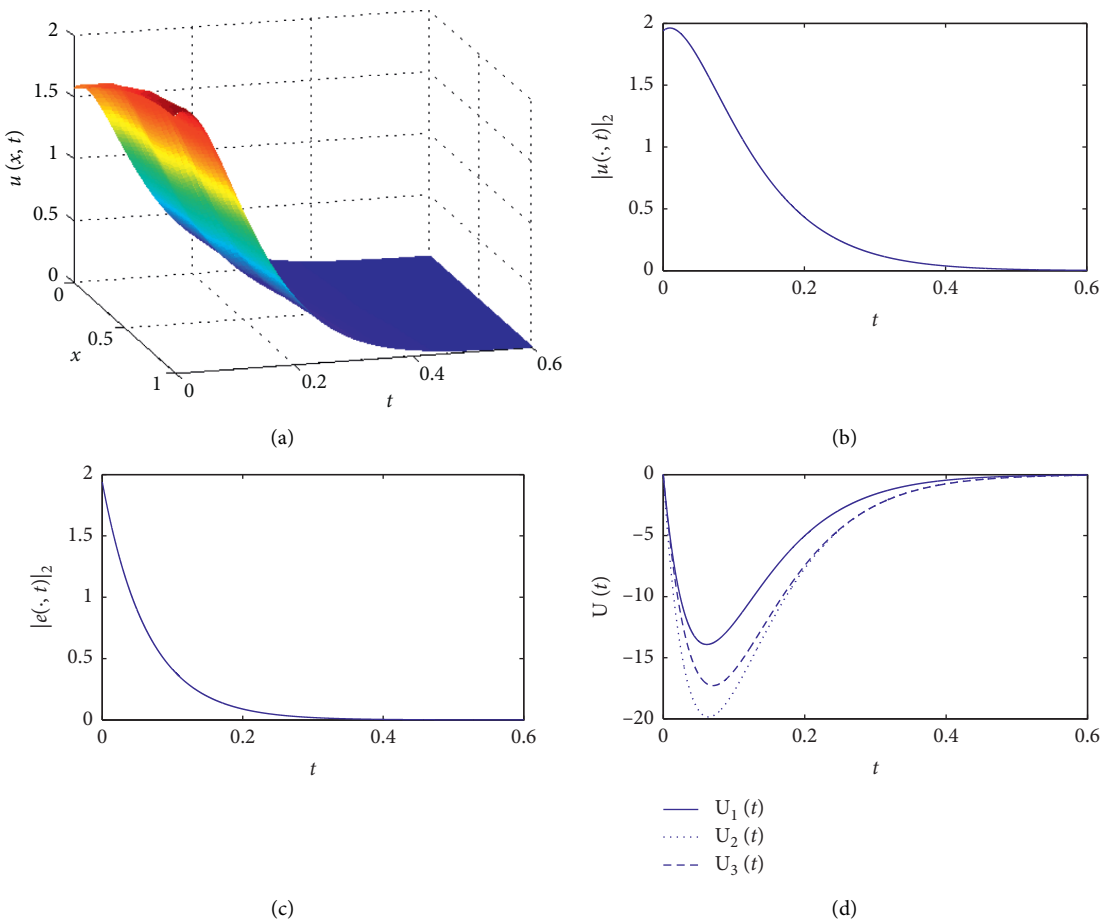

Figure 2: Closed-loop coupled DPS (18), (19), (7), and (9) with $d(z,t) = 0$ and $\omega(t) = 0$ for local piecewise control and noncollocated local piecewise measurement in space. (a) Closed-loop profile of evolution of $u(z,t)$. (b) Closed-loop trajectory of $|u(\cdot,t)|_2$. (c) Closed-loop trajectory of $|e(\cdot,t)|_2$. (d) Trajectory of dynamic output feedback compensator $\mathbf{U}(t)$.

$\varepsilon = 10, r = 0.5$; by solving the LMIs (39) and (40), we get the optimised H_∞ attenuation levels as $\gamma_1 = 20.6102, \gamma_2 = 18.6307$, compensator gains $k_1 = 52.1015$, $k_2 = 71.7887$, and $k_3 = 52.1015$, and observer gains $l_1 = 77.0853, l_2 = 69.8957$. Applying the designed observer-based dynamic output feedback compensator (15) with the calculated compensator gains and observer gains, the closed-loop profile of evolution of $u(z,t)$, the closed-loop trajectory of $|u(\cdot,t)|_2$, $|e(\cdot,t)|_2$,

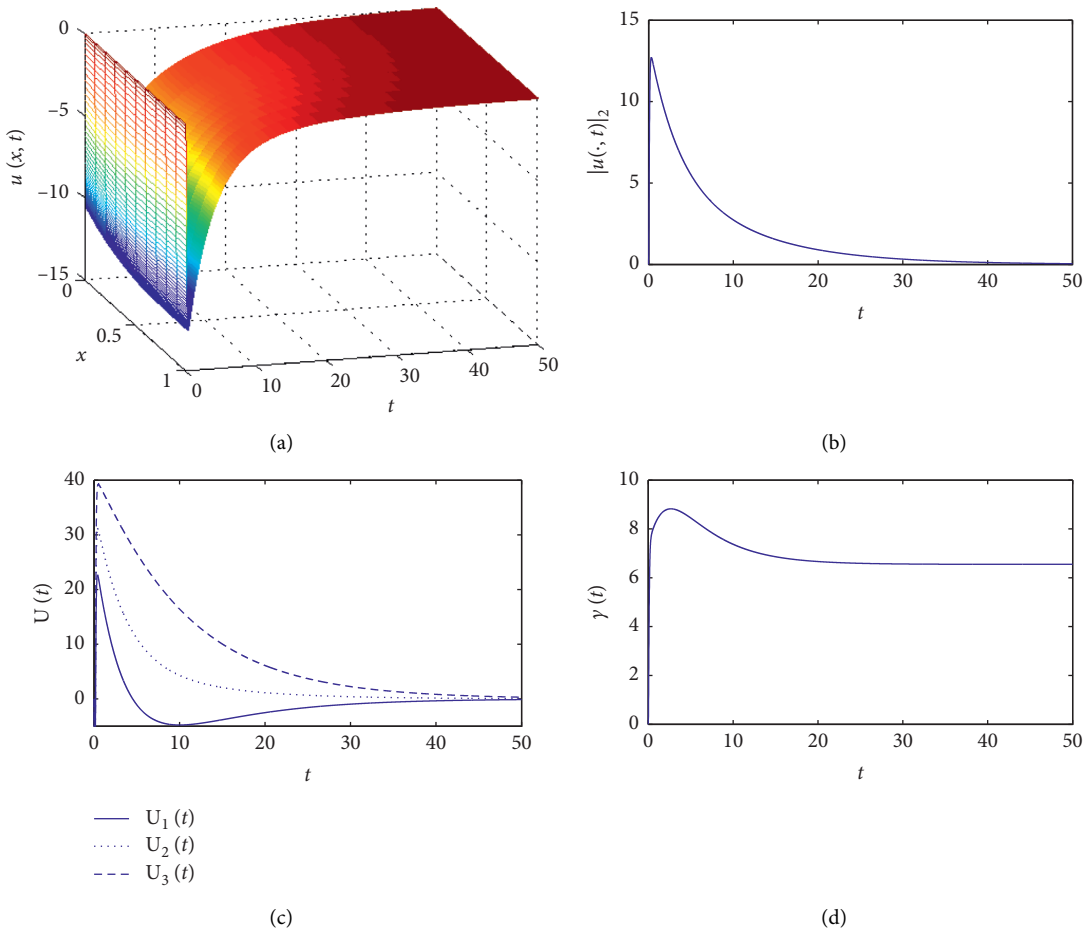

Figure 3: Closed-loop coupled DPS (18), (19), (7), and (9) with $u_0(\cdot) = 0$ and $d(z,t) = \cos(\pi x)\exp(-t)$, $\omega(t) \triangleq [\exp(-0.1t) \;\; \exp(-0.3t)]$, for local piecewise control and noncollocated local piecewise measurement in space. (a) Closed-loop profile of evolution of $u(z,t)$. (b) Closed-loop trajectory of $|u(\cdot,t)|_2$. (c) Trajectory of observer-based dynamic output feedback compensator $\mathbf{U}(t)$. (d) The trajectory of $\gamma(t)$.

and the trajectory of the observer-based dynamic output feedback compensator $\mathbf{U}(t)$ of the form (15) with $d(z,t) = 0$, $\omega(t) = 0$ are shown in Figure 2. The simulation results indicate that the designed observer-based dynamic output feedback compensator (15) can stabilize the MIMO PDE (1)–(3) with $d(\cdot,t) = 0, \omega(t) = 0$ in the sense of $|\cdot|_2$.

Figure 3 presents the closed-loop profile of evolution of $u(z,t)$, the closed-loop trajectory of $|u(\cdot,t)|_2$, the observer-based dynamic output feedback compensator $\mathbf{U}(t)$ in (14), and the trajectory of $\gamma(t)$ for the closed-loop coupled DPS (18), (19), (7), and (9) with $u_0(\cdot) = 0$ and $d(z,t) = \cos(\pi x)$ $\exp(-t)$, $\omega(t) \triangleq [\exp(-0.1t) \;\; \exp(-0.3t)]$. It is easily seen from Figure 3 that $\gamma(t) < \min\{\gamma_1, \gamma_2\}$, which implies $\int_0^\infty |u(\cdot,t)|_2^2 \mathrm{d}t \le \gamma_1^2 \int_0^\infty |d(\cdot,t)|_2^2 \mathrm{d}t + \gamma_2^2 \int_0^\infty \|\omega(t)\|^2 \mathrm{d}t$; the H_∞ performance constraint (10) is guaranteed. The simulation results indicate that the designed observer-based dynamic output feedback compensator (15) can stabilize the linear parabolic DPS (1)–(3) with $u_0(\cdot) = 0$ and $d(z,t) = \cos(\pi x)\exp(-t)$, $\omega(t) \triangleq [\exp(-0.1t) \;\; \exp(-0.3t)]$, in the sense of $|\cdot|_2$.

5. Conclusions

In this paper, the robust H_∞ feedback compensator for a class of linear parabolic DPSs with external disturbances has been investigated in consideration of the pointwise/piecewise control and pointwise/piecewise measurement based on the distributions of the actuators and sensors. A new type of Luenberger observer is designed to solve the difficulty caused by noncollocated observation and track the state of the PDEs. It is different from the previous observer design method that all the cases of the pointwise/piecewise control and pointwise/piecewise measurement are considered via a defined unified distribution function. An observer-based dynamic output feedback compensator is designed and an H_∞ performance constraint is proposed under the zero initial condition. By utilizing Poincaré–Wirtinger inequality's variants, Cauchy–Schwartz inequality, integration by parts, and first mean value theorem for definite integrals, sufficient conditions on the exponential stability of the corresponding closed-loop system under an H_∞

performance constraint in the sense of $|\cdot|_2$ are presented in terms of LMI constraints. Finally, numerical simulation results of the resulting closed-loop systems are provided to illustrate the effectiveness of the proposed design strategy.

Data Availability

The data of this paper come from the official website of sample enterprises, which can be obtained.

Conflicts of Interest

The authors declare that they have no conflicts of interest.

Acknowledgments

This work was supported in part by the Grants of National Key R&D Program of China (2020AAA0108304), National Natural Science Foundation of China (62003275, U1911401, 62073088, and U1701261), Fundamental Research Funds for the Central Universities of China with Grant (31020190QD039), Guangdong Basic and Applied Basic Research Foundation (2019A1515011606), and Guangdong Provincial Key Laboratory of Electronic Information Products Reliability Technology (2017B030314151).

References

[1] P. D. Christofides, *Nonlinear and Robust Control of PDE Systems: Methods and Applications to Transport-Reaction Processes*, Birkhauser, Boston, MA, USA, 2001.

[2] H.-X. Li and C. Qi, *Spatio-Temporal Modeling of Nonlinear Distributed Parameter Systems: A Time/Space Separation Based Approach*, Spinger-Verlag, Amsterdam, The Netherlands, 2011.

[3] K.-K. Xu, H.-X. Li, and H.-D. Yang, "Local-properties-embedding-based nonlinear spatiotemporal modeling for lithium-ion battery thermal process," *IEEE Transactions on Industrial Electronics*, vol. 65, no. 12, pp. 9767–9776, 2018.

[4] B. Roffel and B. H. Betlem, *Advanced Practical Process Control*, Springer, Berlin, Germany, 2004.

[5] R. Padhi and S. F. Ali, "An account of chronological developments in control of distributed parameter systems," *Annual Reviews in Control*, vol. 33, no. 1, pp. 59–68, 2009.

[6] B. Luo, H.-N. Wu, and H.-X. Li, "Adaptive optimal control of highly dissipative nonlinear spatially distributed processes with neuro-dynamic programming," *IEEE Transactions on Neural Networks and Learning Systems*, vol. 26, no. 4, pp. 684–696, 2014.

[7] Z.-P. Wang and H.-N. Wu, "Finite dimensional guaranteed cost sampled-data fuzzy control for a class of nonlinear distributed parameter systems," *Information Sciences*, vol. 327, pp. 21–39, 2016.

[8] W. He, T. Meng, X. He, and S. S. Ge, "Unified iterative learning control for flexible structures with input constraints," *Automatica*, vol. 96, pp. 326–336, 2018.

[9] W. He, T. Meng, X. He, and C. Sun, "Iterative learning control for a flapping wing micro aerial vehicle under distributed disturbances," *IEEE Transactions on Cybernetics*, vol. 49, no. 4, pp. 1524–1535, 2018.

[10] W. Kang and E. Fridman, "Distributed sampled-data control of Kuramoto-Sivashinsky equation," *Automatica*, vol. 95, pp. 514–524, 2018.

[11] Z.-P. Wang and H.-N. Wu, "Sampled-data fuzzy control with guaranteed cost for nonlinear parabolic PDE systems via static output feedback," *IEEE Transactions on Fuzzy Systems*, vol. 28, no. 10, pp. 2452–2465, 2019.

[12] R. Wang, C. Wang, H. Sun, Z. Chen, and Y. Sun, "Sensor fault signal reconstruction based on sliding mode observer for flight control systems," *International Journal of Modelling, Identification and Control*, vol. 32, no. 3-4, pp. 204–211, 2019.

[13] Z.-P. Wang, H.-N. Wu, and H.-X. Li, "Fuzzy control under spatially local averaged measurements for nonlinear distributed parameter systems with time-varying delay," *IEEE Transactions on Cybernetics*, vol. 51, no. 3, pp. 1359–1369, 2019.

[14] S.-H. Tsai, J.-W. Wang, E.-S. Song, and H.-K. Lam, "Robust H_∞ control for nonlinear hyperbolic PDE systems based on the polynomial fuzzy model," *IEEE Transactions on Cybernetics*, 2019.

[15] Z. Li, Q. Cai, Z. Ren, H. Zhang, M. Fu, and Z. Wu, "Optimal control of a class of semi-linear stochastic evolution equations with applications," *IET Control Theory & Applications*, vol. 13, no. 4, pp. 602–608, 2019.

[16] Y. Li, C.-Y. Chen, and C. Li, "Stochastic stability criteria for neutral distributed parameter systems with markovian jump," *Complexity*, vol. 2020, Article ID 9450786, , 2020.

[17] Z.-P. Wang, H.-N. Wu, and T. Huang, "Sampled-data fuzzy control for nonlinear delayed distributed parameter systems," *IEEE Transactions on Fuzzy Systems*, 2020.

[18] W. He, X. He, M. Zou, and H. Li, "Pde model-based boundary control design for a flexible robotic manipulator with input backlash," *IEEE Transactions on Control Systems Technology*, vol. 27, no. 2, pp. 790–797, 2018.

[19] W. He, H. Gao, C. Zhou, C. Yang, and Z. Li, "Reinforcement learning control of a flexible two-link manipulator: an experimental investigation," *IEEE Transactions on Systems, Man, and Cybernetics: Systems*, 2020.

[20] W. He, T. Wang, X. He, L.-J. Yang, and O. Kaynak, "Dynamical modeling and boundary vibration control of a rigid-flexible wing system," *IEEE/ASME Transactions on Mechatronics*, vol. 25, no. 6, pp. 2711–2721, 2020.

[21] Z. Zhao, C. K. Ahn, and H.-X. Li, "Boundary anti-disturbance control of a spatially nonlinear flexible string system," *IEEE Transactions on Industrial Electronics*, vol. 67, no. 6, pp. 4846–4856, 2019.

[22] Z. Zhao, X. He, Z. Ren, and G. Wen, "Boundary adaptive robust control of a flexible riser system with input nonlinearities," *IEEE Transactions on Systems, Man, and Cybernetics: Systems*, vol. 49, no. 10, 2018.

[23] J.-W. Wang, Y.-Q. Liu, and C.-Y. Sun, "Adaptive neural boundary control design for nonlinear flexible distributed parameter systems," *IEEE Transactions on Control Systems Technology*, vol. 27, no. 5, pp. 2085–2099, 2018.

[24] R. Vazquez and M. Krstic, "Control of 1-d parabolic PDEs with volterra nonlinearities, part i: design," *Automatica*, vol. 44, no. 11, pp. 2778–2790, 2008.

[25] B.-Z. Guo and W. Guo, "The strong stabilization of a one-dimensional wave equation by non-collocated dynamic boundary feedback control," *Automatica*, vol. 45, no. 3, pp. 790–797, 2009.

[26] M. Krstic, B.-Z. Guo, A. Balogh, and A. Smyshlyaev, "Control of a tip-force destabilized shear beam by observer-based boundary feedback," *SIAM Journal on Control and Optimization*, vol. 47, no. 2, pp. 553–574, 2008.

[27] M. Cheng, V. Radisavljevic, C. Chang, C. Lin, and W. Su, "A sampled-data singularly perturbed boundary control for a

heat conduction system with noncollocated observation," *IEEE Transactions on Automatic Control*, vol. 54, no. 6, pp. 1305–1310, 2009.

[28] M.-B. Cheng, V. Radisavljevic, and W.-C. Su, "Sliding mode boundary control of a parabolic PDE system with parameter variations and boundary uncertainties," *Automatica*, vol. 47, no. 2, pp. 381–387, 2011.

[29] H.-N. Wu, J.-W. Wang, and H.-X. Li, "Fuzzy boundary control design for a class of nonlinear parabolic distributed parameter systems," *IEEE Transactions on Fuzzy Systems*, vol. 22, no. 3, pp. 642–652, 2014.

[30] X. Song, M. Wang, S. Song, and J. Man, "Dissipativity-based controller design for time-delayed ts fuzzy switched distributed parameter systems," *Complexity*, vol. 2018, Article ID 6215945, , 2018.

[31] E. Fridman and Y. Orlov, "An lmi approach to H_∞ boundary control of semilinear parabolic and hyperbolic systems," *Automatica*, vol. 45, no. 9, pp. 2060–2066, 2009.

[32] J.-W. Wang, H.-X. Li, and H.-N. Wu, "A membership-function-dependent approach to design fuzzy pointwise state feedback controller for nonlinear parabolic distributed parameter systems with spatially discrete actuators," *IEEE Transactions on Systems, Man, and Cybernetics: Systems*, vol. 47, no. 7, pp. 1486–1499, 2017.

[33] J.-W. Wang and H.-N. Wu, "Exponential pointwise stabilization of semilinear parabolic distributed parameter systems via the takagi-sugeno fuzzy PDE model," *IEEE Transactions on Fuzzy Systems*, vol. 26, no. 1, pp. 155–173, 2018.

[34] J.-W. Wang and H.-N. Wu, "Design of suboptimal local piecewise fuzzy controller with multiple constraints for quasi-linear spatiotemporal dynamic systems," *IEEE Transactions on Cybernetics*, 2019.

[35] E. Fridman and N. B. Am, "Sampled-data distributed H_∞ control of transport reaction systems control of transport reaction systems," *SIAM Journal on Control and Optimization*, vol. 51, no. 2, pp. 1500–1527, 2013.

[36] E. Fridman and A. Blighovsky, "Robust sampled-data control of a class of semilinear parabolic systems," *Automatica*, vol. 48, no. 5, pp. 826–836, 2012.

[37] M. A. Demetriou, "Guidance of mobile actuator-plus-sensor networks for improved control and estimation of distributed parameter systems," *IEEE Transactions on Automatic Control*, vol. 55, no. 7, pp. 1570–1584, 2010.

[38] M. A. Demetriou, "Adaptive control of 2-d PDEs using mobile collocated actuator/sensor pairs with augmented vehicle dynamics," *IEEE Transactions on Automatic Control*, vol. 57, no. 12, pp. 2979–2993, 2012.

[39] J.-W. Wang and H.-N. Wu, "Lyapunov-based design of locally collocated controllers for semi-linear parabolic PDE systems," *Journal of the Franklin Institute*, vol. 351, no. 1, pp. 429–441, 2014.

[40] A. Selivanov and E. Fridman, "Sampled-data relay control of diffusion PDEs," *Automatica*, vol. 82, pp. 59–68, 2017.

[41] W.-H. Chen, S. Luo, and W. X. Zheng, "Sampled-data distributed H_∞ control of a class of 1-D parabolic systems under spatially point measurements control of a class of 1-d parabolic systems under spatially point measurements," *Journal of the Franklin Institute*, vol. 354, no. 1, pp. 197–214, 2017.

[42] J.-W. Wang, S.-H. Tsai, H.-X. Li, and H.-K. Lam, "Spatially piecewise fuzzy control design for sampled-data exponential stabilization of semilinear parabolic PDE systems," *IEEE Transactions on Fuzzy Systems*, vol. 26, no. 5, pp. 2967–2980, 2018.

[43] J. W. Wang, Y. Q. Liu, and C. Y. Sun, "Observer-based dynamic local piecewise control of a linear parabolic PDE using non-collocated local piecewise observation," *IET Control Theory & Applications*, vol. 12, no. 3, pp. 346–358, 2018.

[44] J.-W. Wang, Y.-Q. Liu, and C.-Y. Sun, "Pointwise exponential stabilization of a linear parabolic PDE system using non-collocated pointwise observation," *Automatica*, vol. 93, pp. 197–210, 2018.

[45] Y. Q. Liu, J. W. Wang, and C. Y. Sun, "Observer-based output feedback compensator design for linear parabolic PDEs with local piecewise control and pointwise observation in space," *IET Control Theory & Applications*, vol. 12, no. 13, pp. 1812–1821, 2018.

[46] H.-N. Wu and Z.-P. Wang, "Observer-based H_∞ sampled-data fuzzy control for a class of nonlinear parabolic PDE systems sampled-data fuzzy control for a class of nonlinear parabolic PDE systems," *IEEE Transactions on Fuzzy Systems*, vol. 26, no. 2, pp. 454–473, 2018.

[47] J.-W. Wang and J.-M. Wang, "Dynamic compensator design of linear parabolic mimo PDEs in n-dimensional spatial domain," *IEEE Transactions on Automatic Control*, vol. 66, no. 3, pp. 1399–1406, 2020.

[48] W. Youn and H. Myung, "Robust interacting multiple model with modeling uncertainties for maneuvering target tracking," *IEEE Access*, vol. 7, pp. 65427–65443, 2019.

[49] J. Xue-bo, L. Xiao-feng, S. Ting-li, S. Yan, and M. Bei-bei, "Closed-loop estimation for randomly sampled measurements in target tracking system," *Mathematical Problems in Engineering*, vol. 2014, Article ID 315908, , 2014.

[50] H. Zhang, X. Zhou, Z. Wang, and H. Yan, "Maneuvering target tracking with event-based mixture kalman filter in mobile sensor networks," *IEEE Transactions on Cybernetics*, vol. 50, no. 10, pp. 4346–4357, 2019.

[51] X. Zhang, F. Ding, and E. Yang, "State estimation for bilinear systems through minimizing the covariance matrix of the state estimation errors," *International Journal of Adaptive Control and Signal Processing*, vol. 33, no. 7, pp. 1157–1173, 2019.

[52] X. Zhang and F. Ding, "Hierarchical parameter and state estimation for bilinear systems," *International Journal of Systems Science*, vol. 51, no. 2, pp. 275–290, 2020.

[53] F. Ding, "State filtering and parameter estimation for state space systems with scarce measurements," *Signal Processing*, vol. 104, pp. 369–380, 2014.

[54] F. Ding, X. Zhang, and L. Xu, "The innovation algorithms for multivariable state-space models," *International Journal of Adaptive Control and Signal Processing*, vol. 33, no. 11, pp. 1601–1618, 2019.

[55] X. Zhang and F. Ding, "Adaptive parameter estimation for a general dynamical system with unknown states," *International Journal of Robust and Nonlinear Control*, vol. 30, no. 4, pp. 1351–1372, 2020.

[56] X. Zhang, F. Ding, and L. Xu, "Recursive parameter estimation methods and convergence analysis for a special class of nonlinear systems," *International Journal of Robust and Nonlinear Control*, vol. 30, no. 4, pp. 1373–1393, 2020.

[57] F. Ding, L. Xu, D. Meng, X.-B. Jin, A. Alsaedi, and T. Hayat, "Gradient estimation algorithms for the parameter identification of bilinear systems using the auxiliary model," *Journal of Computational and Applied Mathematics*, vol. 369, Article ID 112575, 2020.

[58] F. Ding, L. Lv, J. Pan, X. Wan, and X.-B. Jin, "Two-stage gradient-based iterative estimation methods for controlled autoregressive systems using the measurement data,"

International Journal of Control, Automation and Systems, vol. 88, pp. 886–896, 2019.

[59] R. Wang, Y. Li, H. Sun, Y. Zhang, and Y. Sun, "Performance analysis of switched control systems under common-source digital upsets modeled by MDHMM," *Complexity*, vol. 2018, Article ID 4329053, , 2018.

[60] R. Wang, P. Du, W. Zhong, H. Han, and H. Sun, "Analyses and encryption implementation of a new chaotic system based on semitensor product," *Complexity*, vol. 2020, Article ID 1230804, , 2020.

[61] X.-B. Jin, H.-X. Wang, X.-Y. Wang, Y.-T. Bai, T.-L. Su, and J.-L. Kong, "Deep-learning prediction model with serial two-level decomposition based on bayesian optimization," *Complexity*, vol. 2020, Article ID 4346893, , 2020.

[62] J. Pan, H. Ma, X. Jiang, W. Ding, and F. Ding, "Adaptive gradient-based iterative algorithm for multivariable controlled autoregressive moving average systems using the data filtering technique," *Complexity*, vol. 2018, Article ID 9598307, , 2018.

[63] H. Wu and H. Li, "H_∞ Fuzzy observer-based control for a class of nonlinear distributed parameter systems with control constraints," *IEEE Transactions on Fuzzy Systems*, vol. 16, no. 2, pp. 502–516, 2008.

[64] B. Luo, T. Huang, H.-N. Wu, and X. Yang, "Data-driven H_∞ control for nonlinear distributed parameter systems control for nonlinear distributed parameter systems," *IEEE Transactions on Neural Networks and Learning Systems*, vol. 26, no. 11, pp. 2949–2961, 2015.

[65] J.-W. Wang and J.-M. Wang, "Mixed H_2/H_∞ sampled-data output feedback control design for a semi-linear parabolic PDE in the sense of spatial L∞ norm h_2/H_∞ sampled-data output feedback control design for a semi-linear parabolic pde in the sense of spatial l_∞ norm," *Automatica*, vol. 103, pp. 282–293, 2019.

[66] J.-W. Wang, "A unified lyapunov-based design for a dynamic compensator of linear parabolic mimo PDEs," *International Journal of Control*, pp. 1–8, 2019.

[67] Y. Liu and C. Sun, "H_∞ piecewise control for linear parabolic distributed parameter systems with piecewise observation in space piecewise control for linear parabolic distributed parameter systems with piecewise observation in space," *IEEE Access*, vol. 7, pp. 62865–62874, 2019.

[68] J.-W. Wang, "Exponentially stabilizing observer-based feedback control of a sampled-data linear parabolic multiple-input-multiple-output pde," *IEEE Transactions on Systems, Man, and Cybernetics: Systems*, 2019.

[69] V. Balakrishnan, "All about the Dirac delta function (?)," *Resonance*, vol. 8, no. 8, pp. 48–58, 2003.

[70] M. Krstic and A. Smyshlyaev, *Boundary Control of PDEs: A Course on Backstepping Designs*, SIAM, Philadephia, PA, USA, 2008.